Multi-elemental Characterization of Soils in the Vicinity of Siderurgical Industry: Levels, Depth Migration and Toxic Risk

Antoaneta Ene * , Florin Sloată , Marina V. Frontasyeva , Octavian G. Duliu , Alina Sion , Steluta Gosav , Diana Persa

Posted Date: 10 April 2024

doi: 10.20944/preprints202404.0668.v1

Keywords: soils; siderurgy; metals; trace elements; contamination; INAA; toxic risk

 doi:10.20944/preprints202404.0668.v1

Article

Multi-Elemental Characterization of Soils in the Vicinity of Siderurgical Industry: Levels, Depth Migration and Toxic Risk

Antoaneta Ene [1,*], Florin Sloată [1], Marina V. Frontasyeva [2], Octavian G. Duliu [3,4], Alina Sion [1], Steluta Gosav [1] and Diana Persa [3]

[1] Dunarea de Jos University of Galati, Faculty of Sciences and Environment, Department of Chemistry, Physics and Environment, INPOLDE research center, 47 Domneasca St., 800008 Galati, Romania
[2] Joint Institute for Nuclear Research, 6 Joliot Curie St., 141980 Dubna, Russian Federation
[3] Geological Institute of Romania, 1 Caransebes St., 012271 Bucharest, Romania
[4] University of Bucharest, Faculty of Physics, Department of Structure of Matter, Earth and Atmospheric Physics, Astrophysics, 405 Atomistilor St., 077125 Magurele, Ilfov, Romania
* Correspondence: antoaneta.ene@ugal.ro

Abstract: The assessment of soil contamination in the vicinity of integrated siderurgical plants is of outmost importance for agroecosystems and human health, and sensitive techniques should be employed for accurate assessment of chemical elements (metals, potential toxic elements, rare earths, radioelements) in soil and further evaluation of potential ecological and safety risk. In this paper a total of 45 major, minor and trace elements (Al, As, Au, Ba, Br, Ca, Cd, Ce, Co, Cr, Cs, Cu, Dy, Eu, Fe, Hf, Hg, I, K, La, Mg, Mn, Mo, Na, Nd, Ni, Pb, Rb, Sb, Sc, Sm, Sn, Sr, Ta, Tb, Th, Ti, Tm, U, V, W, Y, Yb, Zn and Zr) were quantified in soils located around a large siderurgical works (Galati, SE Romania) using instrumental neutron activation analysis (INAA) in combination with X-ray fluorescence (XRF) and inductively coupled plasma mass spectrometry (ICP-MS). The statistical analysis results and vertical distribution patterns for three depths (0-5 cm, 5-20 cm, 20-30 cm) indicate inputs of toxic elements in the sites close to the ironmaking and steelmaking facilities and industrial wastes dumping site. For selected elements, a comparison with historical, legislated and world reported concentration values in soil was performed and depth migration, contamination and toxic risk indices were assessed. The distribution of major, rock forming elements was closer to the Upper Continental Crust (UCC), and to the Dobrogea loess, finding confirmed by the ternary diagram of the incompatible trace elements Sc, La and Th, as well as by the La to Th rate. At the same time, the La/Th vs. Sc and Th/Sc vs. Zr/Sc bi-plots suggested a felsic origin and a weak recycling of soils mineral components.

Keywords: soils; siderurgy; metals; trace elements; contamination; INAA; health risk

1. Introduction

Soil is a vital resource which provides essential support to humans and ecosystems. Industrial activities, such as metal smelting, steel production, mining, chemical industry and coal-fired power production, may cause soil quality degradation and serious pollution of environment with toxic trace elements which could negatively impact human health due to their accumulation, persistence and transfer in the compartments of the food chain [1–5]. The elemental analysis at trace level is an important analytical task in various laboratories and high precision techniques such as Instrumental Neutron Activation Analysis (INAA) [4–10], X-ray Fluorescence (XRF) [9–14] and inductively coupled plasma mass spectrometry (ICP-MS) [9,12–15] have shown to be powerful tools for multielemental analysis of a variety of environmental matrices, including soil and rock material, as

 doi:10.20944/preprints202404.0668.v1

well as for the assessment of mineralogical and geochemical features and spatio-temporal contamination trends of a certain region.

This work was aiming to apply INAA, XRF and ICP-MS in order to examine the soil multi-element load, level of soil pollution with Potential Contaminant Elements (PCEs) and their ecological impact around the largest integrated ferrous (iron and steel) metallurgical plant (ISP) in Romania located at Galati town — the biggest port on the maritime Danube — which is one of the most important integrated complexes in the South-East of Europe (Figure 1) [11,16,17], with a great potential of environmental contamination due to specific emissions from iron smelting, processing of ores, coal and auxiliary materials, agglomeration and sintering, minerals and scrap transportation, steelmaking, etc. [3,18–20]. The importance of the targeted region also derives from its closeness to the Danube River, the confluence of Danube with its main tributaries Siret and Prut Rivers, and proximity to the ecologically valuable natural sites and special protected areas in Romania, Republic of Moldova and Ukraine in the Lower Danube River and Black Sea basins [17,21,22]. The activity of this large ferrous metallurgical facility started in 1965, is continuing today, but in the last decade some of the units (blast furnaces, steelworks and mills) were closed and the slag dumping has stopped [23].

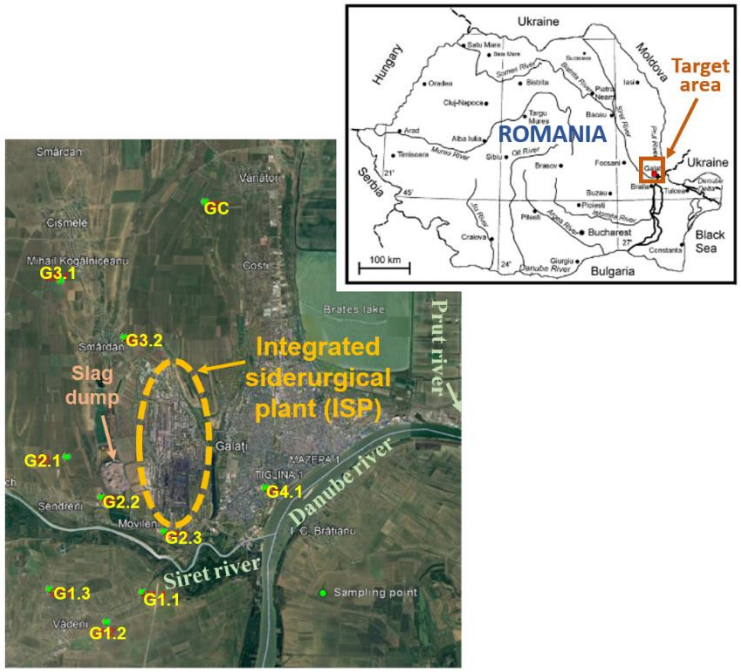

Figure 1. The location of sampling points around the Galati integrated siderurgical plant (ISP). The inset illustrates the position of the investigated area with respect to Romanian territory.

The aim of this paper was two-fold: 1) to study the soil mineralogy, the spatial and depth distribution pattern of 45 major and trace elements in soils belonging to several territorial-administrative units (TAU) of Galati (GL) and Braila (BR) counties in the South–East Development Region of Romania; and 2) to assess the ecotoxicological risk of PCEs in soils adjacent to siderurgical industry, which might produce serious health disorder.

The work was carried out as a continuation and extension of pollution and risk assessment of previous studies limited to soil contamination with heavy metals [4,10,11,16] and persistent organic pollutants (POPs) [17] in Galati industrial area and SE Romania in the period 2005-2009, and in connection with other projects implemented in the frame of international networks, focused on the determination of toxic compounds (heavy metals, radionuclides, POPs, pharmaceutics and endocrine disruptors) and assessment of ecological and human health risk in the Black Sea Basin [3,14,15,22,24].

 doi:10.20944/preprints202404.0668.v1

2. Materials and Methods

2.1. Sampling and Sample Processing

Composite soil samples of about 1.5 kg were collected at nine sites around a large steel plant in SE Romania (Figure 1) from three different layers in the depth intervals: 0–5 cm, 5–20 cm and 20–30 cm. The samples labeled as G1 were taken from the village of Vadeni, Braila County, and the other samples (G2, G3, G4) from Galati County, from localities of Sendreni and Smardan TAUs and Galati town. A control sample (GC) was collected from Vanatori village, in the north part of Galati town (Figure 1). The site description is presented in Table 1.

Table 1. Site description.

Code	Longitude	Latitude	Description
G1.1	45°23'00.4"	27°57'46.2"	TAU Vadeni, BR, rural, S of ISP
G1.2	45°22'22.0"	27°56'40.6"	TAU Vadeni, BR, rural
G1.3	45°23'03.7"	27°54'56.8"	TAU Vadeni, BR, agricultural
G2.1	45°25'53.8"	27°55'28.4"	TAU Sendreni, GL, agricultural, W of slag dump
G2.2	45°25'02.0"	27°56'31.6"	TAU Sendreni, Movileni, GL, rural, SW of slag dump
G2.3	45°24'18.2"	27°58'26.1"	GL town limit, periurban, S of ISP
G3.1	45°29'39.6"	27°55'17.0"	TAU Smardan, Mihail Kogalniceanu, GL, rural, N of ISP
G3.2	45°28'27.0"	27°57'13.7"	TAU Smardan, GL, agricultural, N of ISP
G4.1	45°25'14.1"	28°01'31.3"	GL town, urban, E of ISP
GC	45°31'20.5"	27°59'41.6"	TAU Vanatori, GL, control rural site

The collected soil samples were prepared for various analyses at INPOLDE research center, Dunarea de Jos University of Galati, Romania, being cleaned from stones, vegetal material and other debris, dried at room temperature, then grounded and sieved to a granulation of 0.01 mm.

2.2. Analytical Techniques

Two non-destructive analytical techniques were used in this research, such as: epithermal neutron activation analysis (INAA) and X-ray fluorescence (XRF) analysis. The two analysis techniques were used to determine with high accuracy and precision the total concentrations of 44 major, minor and trace elements (INAA— Na, Mg, Al, K, Ca, Ti, V, Cr, Mn, Fe, Ni, Co, Zn, As, Br, Rb, Sr, Zr, Nb, Mo, Sb, I, Cs, Ba, La, Ce, Nd, Sm, Eu, Tb, Dy, Tm, Yb, Hf, Ta, W, Au, Hg, Th and U; XRF— Cu, Pb, Sn, Y) in the soil samples taken around a large steel plant in SE Romania. For Cd analysis, the ICP-MS technique was employed.

The instrumental neutron activation analysis (INAA) analytical technique was applied at REGATA installation of the IBR-2M reactor within the Frank Laboratory of Neutron Physics (FLNP), of Joint Institute for Nuclear Research (JINR) Dubna, Russian Federation. Several channels of the IBR-2M reactor were used, which allowed the irradiation of the samples with thermal and epithermal neutrons. Soil samples weighing around 100 mg, together with certified reference materials, were wrapped in polyethylene bags and aluminium foils for the short and long-term irradiation, respectively, according to the analytical scheme described in other work [7,25–28]. The induced radioactivity in the samples was measured with the aid of gamma spectrometric chains equipped with automatic switch system for soil and standard material samples [7,25]. The gamma spectra were processed using the software developed at JINR [26] and the analysis was performed based on the radionuclides formed in the samples during activation with neutrons with various energies, listed in [5–7,25].

For the application of XRF spectrometric analysis with energy dispersion the prepared samples were put in specific capsules coated with a Myler foil. The encapsulated samples were irradiated for 120 seconds using a portable Genius XRF spectrometer manufactured by Skyray Instruments Inc., equipped with a large area and detector with Be window and an excitation source of 40 kV / 100μA miniature X-ray tube with an Ag-target [14,23].

 doi:10.20944/preprints202404.0668.v1

ICP-MS was applied for cadmium determination with the aid of an Agilent 7700X ICP-MS spectrometer from the International Hellenic University (IHU), Kavala, Greece, a partner laboratory of INPOLDE center in the frame of MONITOX network [24], as described in a previous study [14].

2.3. Depth Migration, Contamination and Toxic Risk Indices

In order to qualitatively assess the degree of migration/mobility in soil of the determined chemical elements, the depth migration index (DMI) was calculated for each element using the Eq. (1), adapted by us after [29,30], for all the depths from which samples were taken (from 0 to 30 cm):

$$DMI = \sum_{i=1}^{n} \left(\frac{c_i}{c_T}\right) D_i \quad (1)$$

where n=3 represents the number of layers from which the samples were taken, c_i is the value of the chemical element concentration in each sampled layer *i*, $c_T = \sum_{i=1}^{n} c_i$ is the sum of the values of the chemical element concentrations from all the depths of the sampled layers, and D_i is the depth (in cm) of the lower limit of each sampled layer (5, 20 or 30 cm). The value of this index ranges from 1 (if the element accumulated entirely in the first cm) to 30 (if the element accumulated entirely between 29 and 30 cm). *The migration/mobility potential is classified into four categories, labelled as: A (DMI<5) — very low; B (5<DMI<10) — moderate; C (10<DMI<20) — high; D (DMI>20) — very high* [16,30].

Contamination factor (CF) for an individual chemical element is defined by Eq. (2) as the ratio of each element concentration in the soil sample to the element concentration in background soil [31]:

$$CF = \frac{c_{sample}}{c_{background}} \quad (2)$$

where c_{sample} and $c_{background}$ are the measured concentration and the background concentration value of metal *i*, respectively. The contamination classification of soils using this index is: CF < 1 – low; 1 ≤ CF < 3 – moderate; 3 ≤ CF < 6 – considerable; CF ≥ 6 – very high [2,31–34].

To evaluate the pollution levels of various contaminants specific to a site, the site Pollution Load Index (PLI) was employed, utilizing Eq. (3) as introduced by Tomlinson et al. (1980) [35]. This equation involves computing the *n*th root of the product of the highest individual contamination factors CF^i, calculated for specific metals (PCEs) which might result from siderurgical industry activity (n=number of elements/ contamination factors). In this work we considered n=13 PCEs, chosen from those specified in the Romanian legislation [36] and probably to be emitted during the iron and steel making and steel products manufacturing processes, e.g. Hg, Cd, As, Pb, Cu, Co, Ni, Cr, Mn, Zn, Fe, V and Sb. The site PLI categories are the following: PLI≤1– unpolluted (Background Pollution); PLI ≥1– polluted.

$$PLI = \left(CF^1 \times CF^2 \times \ldots\ldots\ldots \times CF^n\right)^{1/n} \quad (3)$$

Similar to the definition of the site PLI and classification, a Regional Pollution Load Index (RPLI) is defined in this work with the aid of Eq. 4, as the *m*th root of the product of the individual site average PLIs [35], calculated for the m=9 industrial sites (except for the control site GC) in Galati ISP area,

$$RPLI = \left(PLI^1 \times PLI^2 \times \ldots\ldots\ldots \times PLI^m\right)^{1/m} \quad (4)$$

Ecological risk factor (E_r^i) for an element *i* is defined with the aid of the Eq. (5):

$$E_r^i = T_r^i \times CF^i \quad (5)$$

where the toxic response factors (T_r^i) for the selected toxic trace elements are the following: Hg–40, Cd–30, As–10, Pb–5, Cu–5, Co–5, Ni–5, Cr–2, Mn–1, Zn–1, as indicated in the literature studies [2,31–34,37,38]. The risk classification using this individual ecotoxicological index is: $E_r^i < 40$ – low potential ecological risk; $40 \le E_r^i < 80$ – moderate potential ecological risk; $80 \le E_r^i < 160$ – considerable potential ecological risk; $160 \le E_r^i < 320$ – high potential ecological risk; $E_r^i \ge 320$ – very high potential ecological risk [32].

The risk index RI is the sum of calculated ecological risk factors corresponding to all *n*=10 hazardous elements analyzed, according to Eq. (6):

$$RI = \sum_{i=1}^{n} E_r^i \quad (6)$$

 doi:10.20944/preprints202404.0668.v1

The risk classification using this complex ecotoxicological index is: RI < 90 – low; 90 ≤ RI < 180 – moderate; 180 ≤ RI < 360 – strong; 360 ≤ RI < 720 – very strong; RI ≥ 720 – highly strong [32].

2.4. Mapping and Statistical Data Analysis

Principal Component Analysis (PCA) and Cluster Analysis (CA) – i.e. Joining or Tree Clustering – were applied to examine the relationship among the sampling sites and elemental load for each soil layer. The inputs consisted of 45 variables representing the concentrations for all 45 chemical elements which were determined in soils collected from nine industrial sites surrounding the enterprise and one control site (GC).

The experimental data concerning the spatial distribution of RI as well as PLI values for selected PCEs in all three investigated soil layers were organized in a geospatial data base, further processed ArcMap 10.4 Spatial Analyst [39]. This permitted generating six maps representing the spatial distribution of both RI and site PLI indices.

Due to the fact that the sampling points did not follow a regular network, the entire considered area was decomposed in Thiessen – Voronoi polygons [40,41]. In this case, an inverse distance weighting algorithm [42,43] gave the best results. Due to a reduced number of sampling points and in the absence of a confident data concerning the distribution function of PLI values, the nonparametric ANOVA Tukey, Man-Whitney, Dunnett *post hoc* as well as the Spearman correlation were used to calculate the probabilities the PLI distributions corresponding to the considered three layers are closer.

Further, the Discriminant Analysis (DA) [44] was used to evidentiate at which extent the PLI values of each layer are correlated.

PAST 4.1 [45], TIBCO® Data Science / Statistica™ 10 [46], and OriginLab® OriginPro™ 2021 [47] were used for statistical data analysis, and MS Excel 2019 was employed for experimental data processing and graphing.

3. Results and Discussion

3.1. Concentrations of Elements in Industrial Soils

The results obtained by the combined analytical methods INAA, XRF and ICP-MS highlighted the existence of 45 elements in soils. Figure 2 shows the spatial and depth wise distribution of the element concentrations and Table 2 presents the concentration ranges and average of values obtained in this paper, along with the limits allowed by Romanian norms for trace elements in soil (normal values, low alert and intervention for sensitive use of soil, and high alert and intervention for less sensitive use of soil) [36] and literature data for Earth's crust composition [48].

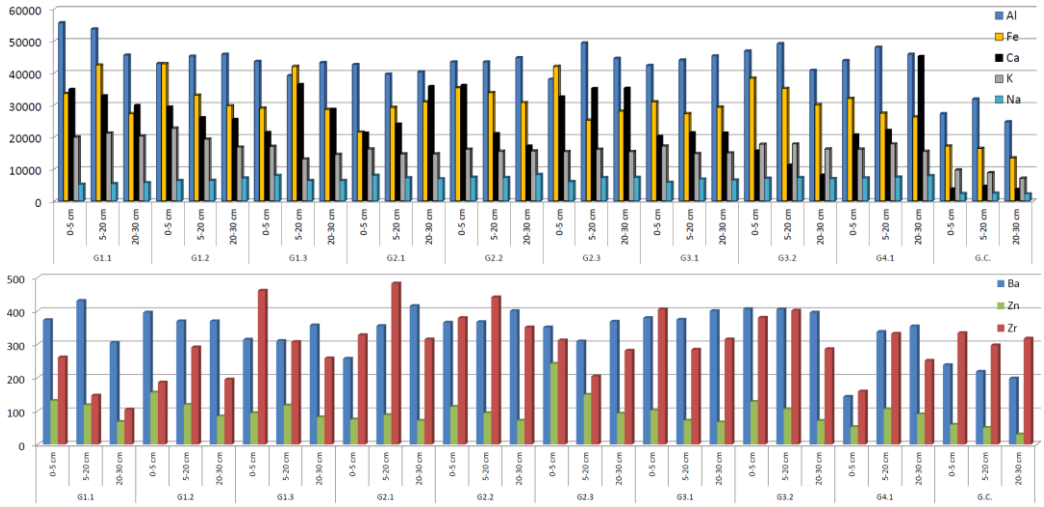

Preprints.org (www.preprints.org) | NOT PEER-REVIEWED | Posted: 10 April 2024 doi:10.20944/preprints202404.0668.v1

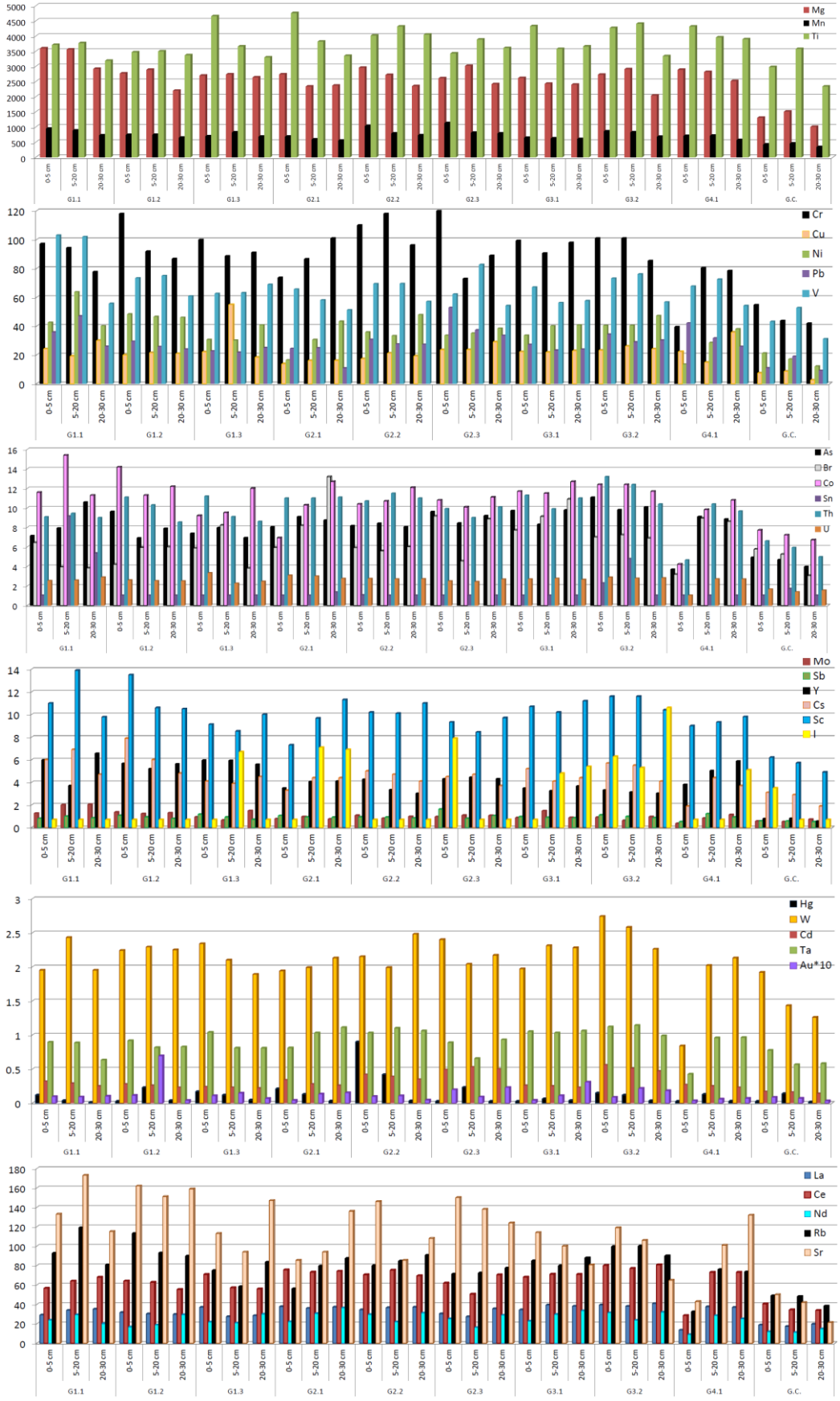

Preprints.org (www.preprints.org) | NOT PEER-REVIEWED | Posted: 10 April 2024 doi:10.20944/preprints202404.0668.v1

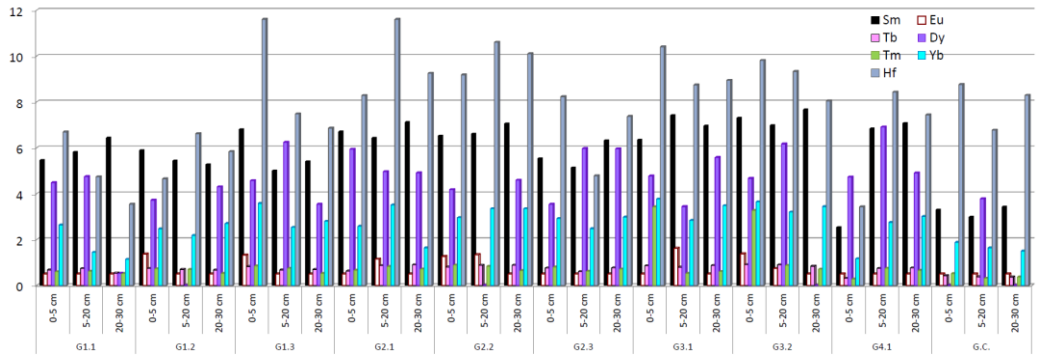

Figure 2. Spatial and depth wise distribution of the element concentrations determined in the investigated soil samples (concentrations on vertical axis are expressed in mg·kg^{-1}).

Table 2. Elemental levels (range, average) in investigated industrial soil samples (except for the control site), norms and Upper Continental Crust (UCC) values, expressed in mg·kg^{-1} (except the major elements, which concentrations are given in g·kg^{-1}, and Au, in µg·kg^{-1}).

	Literature data				This work	
Element	**Normal [36]**	**Low; high – alert [36]**	**Low; high – intervention [36]**	**Upper continental crust mean [48]**	**Galati ISP, min – max**	**Galati ISP, average**
Al, g·kg^{-1}				79.24	38 – 55.6	44.68
As	5	15; 25	25; 50	4.8	3.72 – 11.1	8.55
Au, µg·kg^{-1}				1.5	3.53 – 69.4	10
Ba	200	400; 1000	625; 2000	628	143 – 430	355.6
Br		50; 100	100; 300	1.6	3.19 – 13.2	6.87
Ca, g·kg^{-1}				24.93	10.23 – 47.82	29.26
Cd	1	3; 5	5; 10	0.09	0.22 – 0.56	0.33
Ce				63	28.6 – 80.8	66.65
Co	15	30; 100	50; 250	17.3	4.23 – 15.4	11.08
Cr	30	100; 300	300; 600	92	40 – 120	92.11
Cs				4.9	1.88 – 7.89	4.69
Cu	20	100;250	200;500	28	13.79 – 54.93	23.13

 doi:10.20944/preprints202404.0668.v1

Dy				3.9	n.d. – 6.91	4.20
Eu				1	n.d. – 1.62	0.377
Fe, g·kg^{-1}				38.06	21.5 – 42.8	31.89
Hf				5.3	3.43 – 11.6	7.85
Hg	0.1	1; 4	2; 10	0.05	n.d. – 0.9	0.13
I				1.4	4.82 – 10.6	6.62
K, g·kg^{-1}				25.14	16.73 – 24.42	16.8
La				31	13.6 – 40.9	33.85
Mg, g·kg^{-1}				14.56	2.04 – 3.6	2.7
Mn	900	1500; 2000	2500; 4000	753	554 - 1130	749.5
Mo	2	5; 15	10; 40	1.1	0.37 – 2.04	1.06
Na, g·kg^{-1}				23.57	5.19 – 8.27	6.88
Nd				27	8.9 – 36.4	25.46
Ni	20	75; 200	150; 500	47	13.5 – 63.7	37.99
Pb	20	50; 250	100; 1000	17	10.84 – 52.90	29.40
Rb				84	32.4 – 119	82.53
Sb	5	12.5; 20	20; 40	0.4	0.51 – 1.62	0.95
Sc				14	7.31 – 13.9	10.29
Sm				4.7	2.54 – 7.67	6.23
Sn	20	35; 100	50; 300	2.1	n.d. – 9.16	0.89
Sr				320	43 – 173	117.6

 doi:10.20944/preprints202404.0668.v1

Ta				0.9	0.42 – 1.14	0.925
Tb				0.7	0.31 – 0.91	0.725
Tm				0.3	0.28 – 3.43	0.88
Th				10.5	4.65 – 13.2	10.17
Ti, g·kg^{-1}				3.69	3.19 – 4.76	3.84
U				2.7	1.05 – 3.34	2.651
V	50	100; 200	200; 400	97	51.2 – 103	67.25
W				1.9	0.84 – 2.74	2.14
Y				21	3.04 – 6.58	4.47
Yb				1.96	1.14 – 3.77	2.76
Zn	100	300; 700	600; 1500	67	52.6 – 242	102.26
Zr				193	105 – 482	300.63

n.d. – not detected.

From Figure 2 it can be seen that the highest concentrations of most of the trace elements occur in sites G.2.2. G2.3 and G3.2 which are the closest to the industrial complex, as well as in the location G1.1, situated in the predominant wind direction, trend similar with previous findings for the same industrial area [11,16].

Compared with norms stipulated by Romanian law [36], the concentration values obtained in this work for several PCEs (Table 2) – As, Ba, Co, Cr, Cu, Hg, Mn, Mo, Ni, Pb and Zn – exceed the normal levels, while in the case of Ba, Cr, Pb and V the alert levels are surpassed. With the exception of Al, Ba, Co, K, Mg, Na Sc, Sr and Y, all other major and trace elements are present in the investigated soils in concentrations higher than the Upper Continental Crust (UCC) values [48].

The variation of the depth migration index DMI of identified chemical elements for each sampling location is illustrated in Figure 3.

Preprints.org (www.preprints.org) | NOT PEER-REVIEWED | Posted: 10 April 2024 doi:10.20944/preprints202404.0668.v1

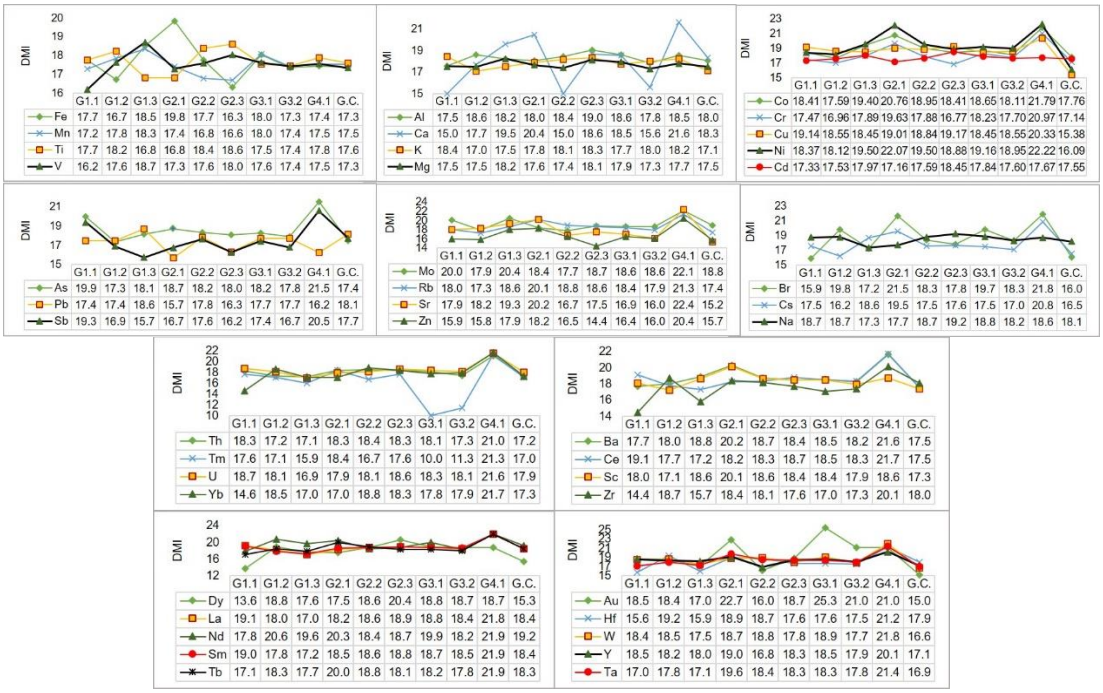

Figure 3. Depth migration index, DMI (cm), of elements in soils around Galati siderurgical plant.

It can be noticed a tendency for element mobilization in the deeper layers of soil, most of the sites being characterized by high (class C) and very high (class D) vertical migration potential; the urban site G4.1. is differing from other locations as being classified with very high migration potential of trace elements, trend also visible in Figure 2 as the elemental levels in the first soil layer are lower than in the second and third layers of this sublocation.

The results for PCA and CA of elemental concentrations are presented in Figures S1 and S2 – Supplementary Material, respectively, for 10 cases (soil sampling sites – 9 industrial sites around Galati integrated siderurgical plant and 1 control site) and 45 variables (concentrations of chemical elements).

PCA results modeled on the basis of the first two most significant principal components (PC1, PC2) specified in Figure S1 are depicted in Figure 4. The PCA shows that as the depth increases the sites are better grouped, with the exception of sites G4.1 for the depth 0-5 cm, respectively G1.1 for the depths 5-20 cm and 20-30 cm. In all cases, it is noticed that the control site GC is distant from the main group, as expected. Similar results were found by applying CA for sites clustering (Figure S2 – Supplementary Material).

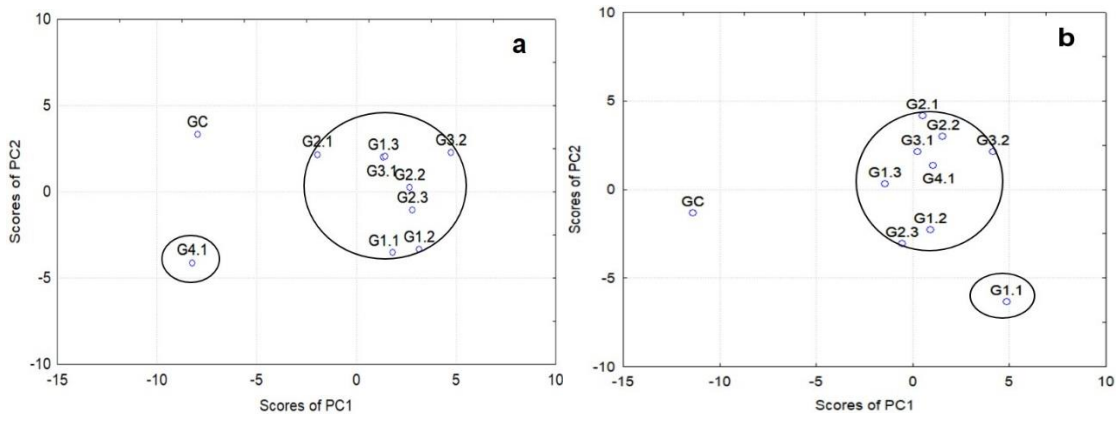

 doi:10.20944/preprints202404.0668.v1

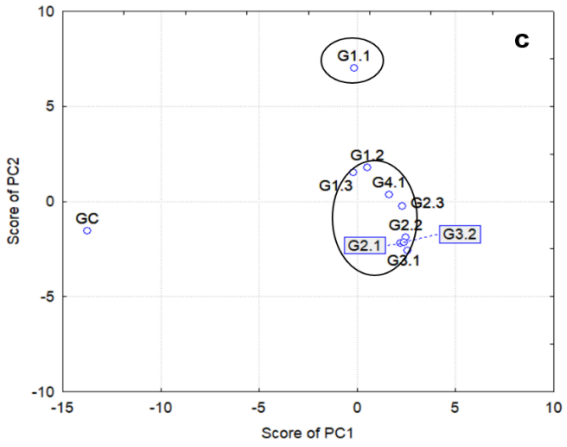

Figure 4. Plot of the PC2 scores as a function of PC1 scores for the soils collected from three depths at the sites around the siderurgical plant and control site: (a) 0–5 cm; (b) 5–20 cm and (c) 20–30 cm.

3.2. Soil Mineralogy

In assessing the origin of the soil mineral component, the incompatible trace elements such as Sc, Co, Zr, rare earth elements (REE), Hf, or Th are very useful [5,8,13]. In this regard, felsic rocks are depleted in Sc but enriched in Th and light REE, while the mafic rocks appear enriched in Sc, Cr, Co, Ni and heavy REE [49]. On this subject, the Sc mass fraction in felsic rocks is less than 20 mg/kg, but exceeds 20-40 mg/kg in mafic rocks so that Sc is one of the most appropriate proxies for such kind of studies [50]. In the case of investigated soils, Sc mass fraction was of 9.8 ± 2 mg/kg. In this regard, the discriminating bi-plot Th/Co vs. La/Sc (Figure 5 a) [51] points with clarity towards a felsic origin of the mineralogy of investigated soil. The presence and distribution of Sc, Zr and Th in the investigated material permitted inferred the past processes that shaped the current situation. Indeed, the mineral zircon due to an extreme resilience to abrasion explained by its hardness on Mohs scale greater than 7.5, showed to be extremely resilient during recycling, so that the higher the Zr mass fraction, the larger the sedimentary material sorting and recycling [52].

Preprints.org (www.preprints.org) | NOT PEER-REVIEWED | Posted: 10 April 2024 doi:10.20944/preprints202404.0668.v1

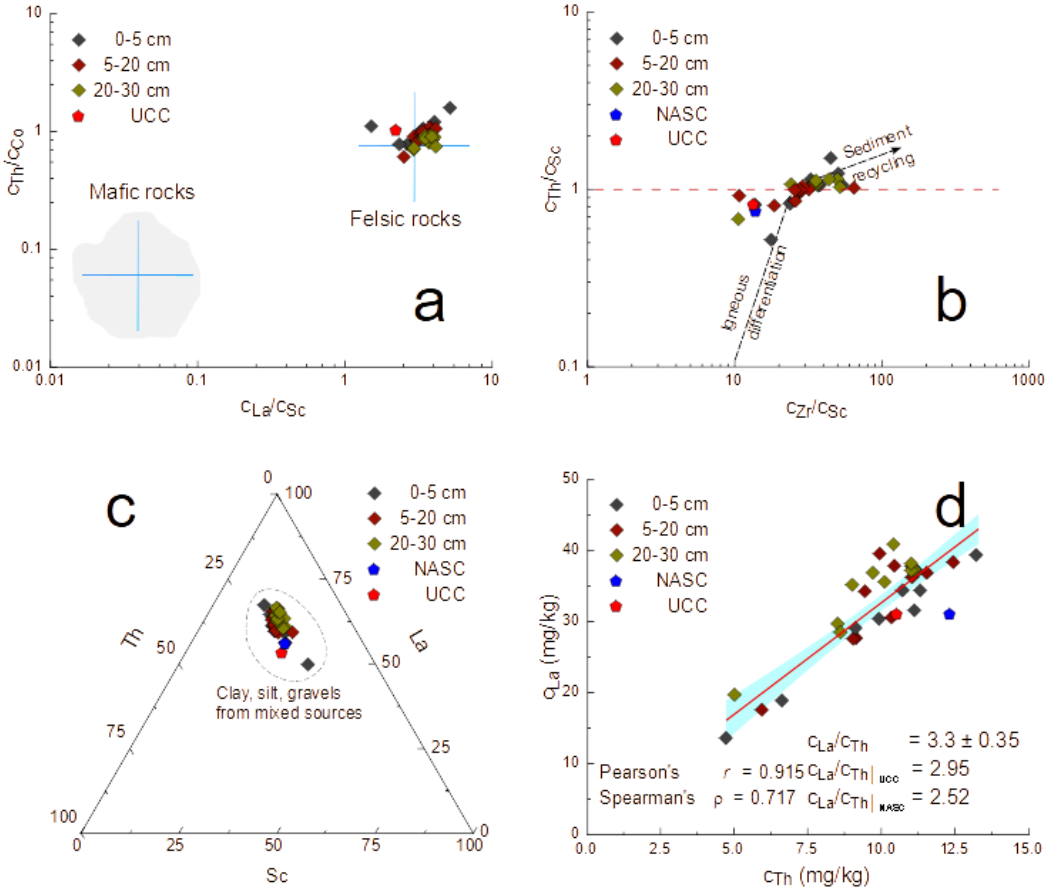

Figure 5. (a) The Th/Co vs. La/Sc discriminating diagrams illustrating the felsic nature of the inorganic/mineral components of investigated soils (a), the Th/Sc vs. Zr/Sc (b) diagram suggesting a reduced recycling of sedimentary material which enters into the soil composition (b) while ternary Sc-La-Th (c) and La vs Th (d) graphics illustrate the closeness of soil mineral components to the Upper Continental Crust (UCC) and the North American Shale Composite (NASC).

In this case, the biplot Th/Sc vs. Zr/Sc showed a relatively reduced recycling when compared with the Dobrogea loess (Figure 5 b) [53], fact explained by the predominance of clastic material in considered soils. More information concerning the affinities of mineral constituents of the soil with the other mineral systems can be furnished, by reciprocal distribution of Sc, La and Th of La and Th [54]. In this regard, both discriminating La-Sc-Th ternary (Figure 5 c) and La vs. Th biplot (Figure 5 d) showed a good correlation between soil inorganic, mineral, component and the Upper Continental Crust (UCC) [48,54] and the North American Shale Composite (NASC) [55].

In the case of Sc-La-Th ternary diagram (Figure 5 c) , all the experimental points corresponding to Galati soils form a cluster around UCC [48,54] and NASC [55], suggesting a composition consisting of clay, silt or gravels from mixed sources. At its turn, the La vs Th bi-plot (Figure 5 d) shows a good correlation between these incompatible elements of which ratio of 3.3 ± 0.35 is close to the UCC one of 2.95 [54] or the NASC value of 2.65 [55]. For this approach to the UCC [48,54] and NASC [55] also pleads the obtained La/Sm mass fractions ratio of 5.47 ± 0.17, close to UCC value of 6.6 [48] and NASC of 5.7 [55].

3.3. Soil Contamination and Ecotoxicological Risk

The second aim of this study consisted of a detailed investigation of 13 PCEs distribution around the Galati integrated steel plant (ISP) given its status of potential contamination source. Accordingly, based on the mass fractions of V, Cr, Mn, Fe, Co, Ni, Cu, Zn, As, Cd, Hg, Sb and Pb determined in soil cores covering the 0-5, 5-20 and 20-30 depth layers, the corresponding PLI (series PLI-13 in Figure 6) was calculated for each sampling point and each layer as one of the most representative

Preprints.org (www.preprints.org) | NOT PEER-REVIEWED | Posted: 10 April 2024 doi:10.20944/preprints202404.0668.v1

contamination index (Figure 6). In the calculations of Contamination Factors (CF) (Table A1, Appendix A), the UCC element concentrations [48] were considered as background values.

Based on the average values of 9 site PLIs, a regional index RPLI of 1.20 was calculated for the metallurgical industrial area of Galati, SE Romania, emphasizing a polluted zone (RPLI >1).

Comparing the PLI values for 13 PCEs with PLI calculated for all 45 identified elements (series PLI-45 in Figure 6), it can be stated that the using of pollutant elements gives rise to relative higher PLI than in the case of considering the elements present at near baseline levels [35], suggesting a real deterioration of soil quality in a region, which is a correct approach.

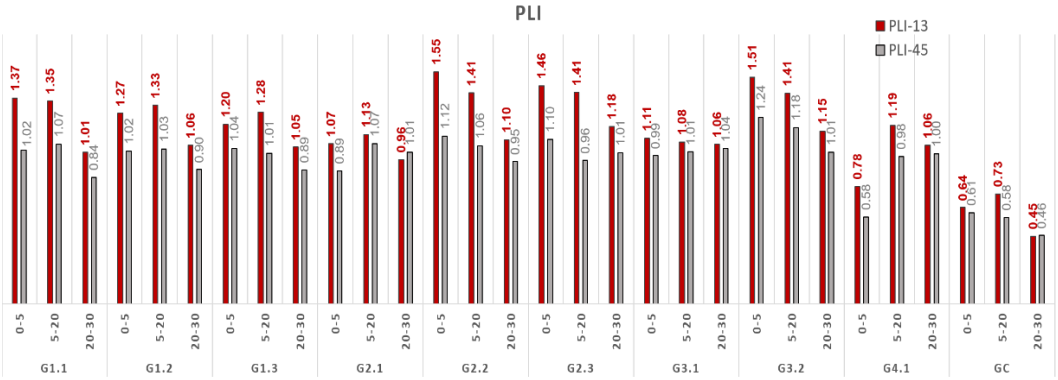

Figure 6. PLI variation with site and depth, calculated for 13 PCEs and 45 elements.

Final results showing the PLI distribution for each sampling point, including the remote one GC, are illustrated by the violin diagram reproduced in Figure 7a. Here it can be remarked that for all three soil layers, the reference one appears less contaminated, fact sustained by PLI values varying between 0.45 and 0.78, i.e. lower than the threshold equal to one necessary to prove a local contamination.

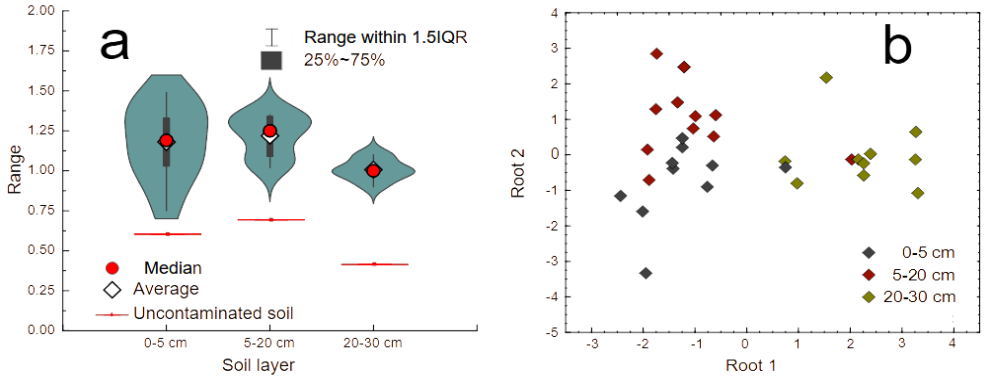

Figure 7. (a) The violin diagram of the distribution of PLI with the depth for contaminated and uncontaminated soil showing the difference between them, as well as (b) the Discriminating bi-plot showing the presence of three clusters consisting of the PLI values corresponding to the three soil layers investigated, i.e. 0-5, 50-20 and 20-30 cm. The partial superposition of the 0-5 and 5-20 cm clusters with respect to the 20-30 cm cluster are visible.

To deepen the study of local contamination we have performed a DA of the PLI values by considering the sampling point as cases and the mass fractions of each of the 13 contaminating elements as variables. The result is reproduced in Figure 7b by a Root 2 vs. Root 1 biplot. This graph shows with clarity the presence of two distinct clusters, one consisting of a partial superposition of the 0-5 and 5-20 cm points and the other one containing only the 20-30 cm data. In our opinion, this

 doi:10.20944/preprints202404.0668.v1

graph suggests that the contamination process is spread onto the 0-20 cm layer while the third layer, between 20 and 30 cm, seems less affected.

This observation is confirmed also by several-samples ANOVA Tukey, Mann-Whitney (Table 3a) and Dunnett post hoc tests, as well as Spearman rank correlation (Table 3b) which showed a certain degree of similitude only between the 0-5 and 5-20 cm layers.

Table 3. The probabilities the distribution of the 13 considered PCE are closer according to Tukey's test (a, lower diagonal), Mann-Whithey (a, upper diagonal), Dunnette *post hoc* (b, lower diagonal) as well as Spearman correlation coefficient (b, upper diagonal).

	a				**b**		
Depth (cm)	0-5	5-20	20-30	depth (cm)	0-5	5-20	20-30
0-5		0.791	0.063	0-5		0.883	0.672
5-20	0.871		0.004	5-20	0.573		0.672
20-30	0.065	0.022		20-30	0.030	0.006	

Another peculiarity can be remarked by analyzing the spatial distribution of PLI corresponding to each of the considered soil layers and illustrated by the maps in Figure 8 (a-c). Here it can be observed that the maximum contamination corresponds to two well evidenced maxima in the sites G2.2 (close to the slag dump) and G3.2 (at the north gate of the enterprise, close to iron scrap deposit, lime factory, steel plant and plate products mills), for which the PLI reaches closer values of 1.55 and 1.51, respectively, for the 0-5 cm layer, closely followed by the G2.3 site (at the south gate of the enterprise, close to agglomeration, sintering and coking plants, blast furnaces and ironmaking facilities) with a PLI value of 1.46. With the depth, these areas enlarge in the second layer (5-20 cm) until they merge in the third layer (20-30 cm), while the maximum PLI values decrease to 1.41 in all three places in the second layer, and 1.10, 1.15, and 1.18, respectively, in the third layer. In our opinion, this finding illustrates a 3D diffusion of contaminating elements into soil starting from the two hotspots better evidenced in Figure 8a.

Three maps were generated representing the spatial distribution of the risk index RI for each soil layer (Figure 8 d-f), calculated in Table 4 for 10 selected PCEs based on the individual ecotoxicological factors E_r^i.

The RI distribution maps highlight the depth diffusion trend of hazardous elements shown by the PLI maps (Figure 8 a-c).

The obtained values for the individual ecotoxicological factors E_r^i and the risk factors RI (Table 4) show that highly ecological risk in the identified industrial hot spots is due to Cd and Hg.

Preprints.org (www.preprints.org) | NOT PEER-REVIEWED | Posted: 10 April 2024 doi:10.20944/preprints202404.0668.v1

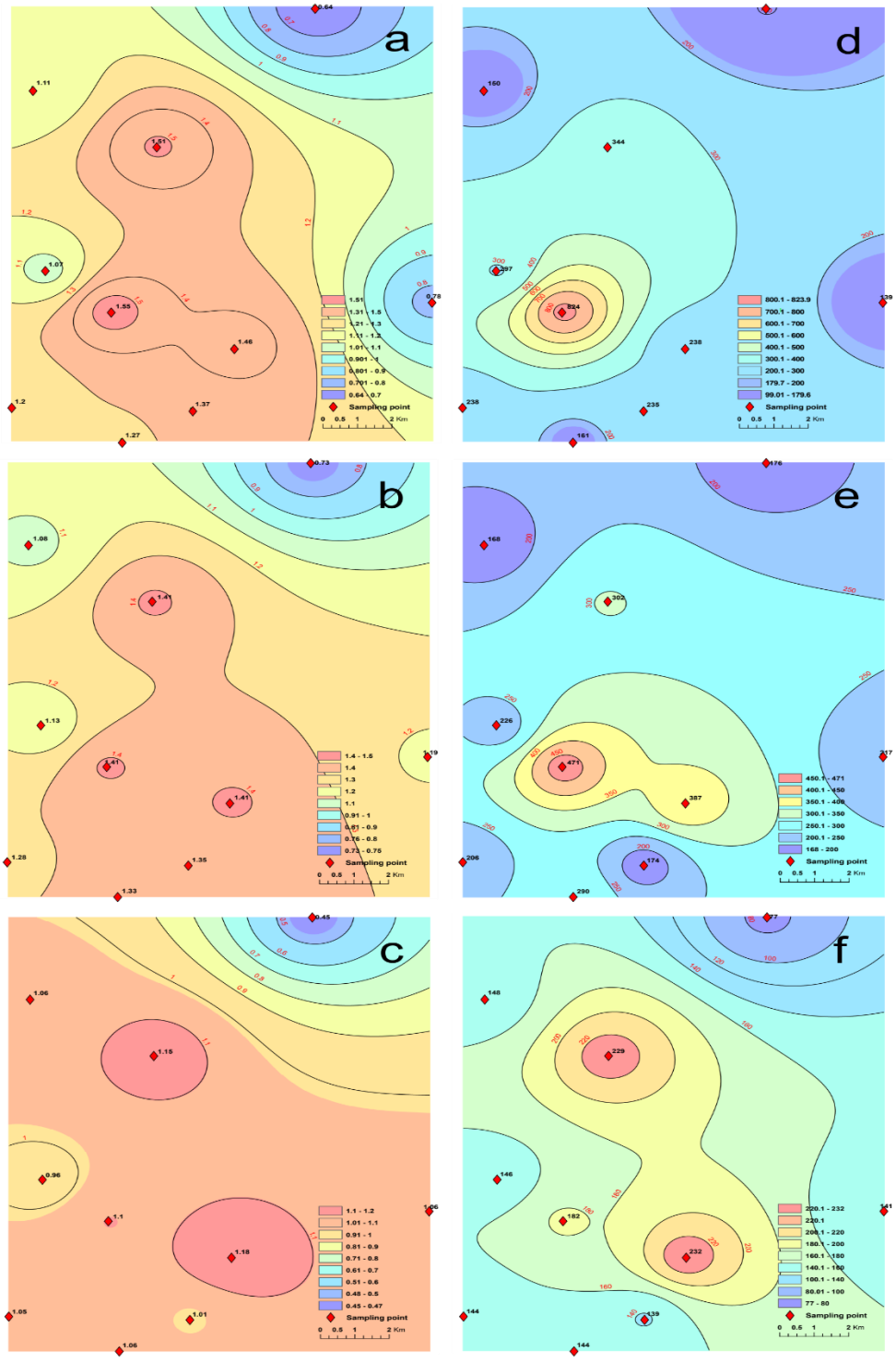

Figure 8. The spatial distribution of the PLI (a-c) and the RI (d-f) corresponding to the 0-5 cm layer (a,d), 5-20 cm layer (b,e), as well as to 20-30 cm layer (c,f).

 doi:10.20944/preprints202404.0668.v1

Table 4. The ecotoxicological factors and risk index of the 10 considered PCEs.

Site code	Depth (cm)	E_r^i										RI
		Hg	As	Pb	Cd	Cu	Cr	Zn	Co	Ni	Mn	
G1.1	0-5	85.71	14.90	10.54	106.67	4.32	2.11	1.96	3.35	4.53	1.26	235.35
	5-20	27.71	16.54	13.84	96.67	3.41	2.05	1.76	4.45	6.78	1.18	174.39
	20-30	9.43	22.08	7.63	83.33	5.35	1.69	1.02	3.27	4.27	0.97	139.03
G1.2	0-5	20.00	20.08	8.63	93.33	3.57	2.57	2.33	4.10	5.14	0.98	160.73
	5-20	164.29	14.42	7.55	86.67	3.85	2.00	1.78	3.27	4.96	0.99	289.75
	20-30	27.57	16.48	7.06	76.67	3.73	1.89	1.26	3.53	4.89	0.86	143.93
G1.3	0-5	121.43	15.40	6.68	80.00	3.95	2.17	1.41	2.66	3.26	0.92	237.88
	5-20	85.71	16.65	6.41	76.67	9.81	1.93	1.75	2.75	3.20	1.09	205.96
	20-30	33.93	14.48	7.33	73.33	3.29	1.98	1.21	3.47	4.34	0.91	144.27
G2.1	0-5	150.00	16.79	7.19	113.33	2.46	1.60	1.12	2.01	1.74	0.91	297.15
	5-20	92.86	18.98	7.29	93.33	2.86	1.88	1.32	2.98	3.26	0.78	225.54
	20-30	22.64	18.23	3.19	86.67	2.88	2.20	1.07	3.67	4.61	0.74	145.88
G2.2	0-5	642.86	17.06	9.02	140.00	3.09	2.39	1.69	3.01	3.81	1.37	824.28
	5-20	300.00	17.56	8.08	130.00	3.79	2.57	1.41	3.09	3.54	1.05	471.09
	20-30	24.00	16.81	8.01	116.67	3.43	2.09	1.07	3.50	5.10	0.97	181.64
G2.3	0-5	20.00	20.04	15.56	163.33	4.21	2.61	3.61	3.12	3.57	1.50	237.56
	5-20	166.43	17.60	10.97	176.67	4.22	1.59	2.22	2.92	3.73	1.08	387.44
	20-30	19.79	19.19	9.86	166.67	5.19	1.93	1.38	3.21	4.09	1.05	232.35
G3.1	0-5	20.00	20.27	7.99	86.67	3.96	2.16	1.52	3.38	3.57	0.86	150.39
	5-20	45.21	17.33	6.83	83.33	3.91	1.97	1.07	3.32	4.27	0.83	168.08
	20-30	28.36	20.40	7.03	76.67	4.08	2.13	1.00	3.67	4.34	0.81	148.48
G3.2	0-5	107.14	23.13	10.08	186.67	4.14	2.20	1.91	3.58	4.30	1.14	344.29
	5-20	85.71	20.44	8.52	170.00	4.66	2.20	1.58	3.58	4.31	1.10	302.09
	20-30	26.07	21.04	8.87	156.67	4.31	1.86	1.06	3.38	5.02	0.90	229.19
G4.1	0-5	20.00	7.75	12.38	90.00	3.98	0.86	0.79	1.22	1.44	0.94	139.35
	5-20	92.86	19.00	9.34	83.33	2.66	1.75	1.58	2.84	3.03	0.95	217.34
	20-30	21.36	18.48	7.59	76.67	6.39	1.71	1.35	3.12	4.04	0.76	141.47
G.C.	0-5	20.00	10.29	3.21	56.67	1.33	1.19	0.89	2.23	2.26	0.56	98.63
	5-20	100.00	9.77	5.60	53.33	1.53	0.95	0.75	2.09	1.82	0.61	176.46
	20-30	14.07	8.31	2.67	46.67	0.46	0.91	0.45	1.95	1.29	0.45	77.22

4. Conclusions

The current study aimed to bring new insights on the quality of soils in the neighborhood of a large siderurgical complex located in Galati, SE region of Romania, regarding the compositional scheme, spatial and depth migration of 45 chemical elements (metals, radioelements, rare earth elements and other trace elements), contamination trends, mineral assemblage, ecotoxicological risk of selected potential contaminant elements and regional contamination level due to industrial activity related to ferrous metallurgy.

Our results obtained for the concentrations and environmental and safety risk indices of elements of concern demonstrate a present pollution of surface layer of soils adjacent to siderurgical industry, although the industrial production and activity had been restrained in the last decade, and a vertical migration of most of the analyzed elements in deeper soil layers.

 doi:10.20944/preprints202404.0668.v1

The geochemical and contamination features suggest a similarity with results obtained in previous surveys performed in Galati industrial area, regarding the location of the impacted sites in dependence of the distance from the enterprise and dominant direction of wind. Our results could constitute a useful database for further investigations in the area and elaboration of land management strategies and exploitation of terrains, as well as decommissioning of the slag dump territory and valorization of metallic materials in various purposes.

Supplementary Materials: The following supporting information can be downloaded at: www.mdpi.com/xxx/s1, Figure S1: Explained variance for the principal components and plot of the PC2 loadings as a function of PC1 loadings; Figure S2: Dendrograms obtained with the Tree Clustering algorithm for the 10 soil samples and 45 variables in three soil layers.

Author Contributions: Conceptualization, Antoaneta Ene and Octavian Duliu; Data curation, Antoaneta Ene and Marina Frontasyeva; Formal analysis, Florin Sloată and Diana Persa; Investigation, Antoaneta Ene, Florin Sloată, Marina Frontasyeva, Alina Sion, Steluta Gosav and Diana Persa; Methodology, Antoaneta Ene, Florin Sloată, Marina Frontasyeva, Octavian Duliu, Alina Sion and Steluta Gosav; Project administration, Antoaneta Ene and Marina Frontasyeva; Resources, Antoaneta Ene; Software, Octavian Duliu, Steluta Gosav and Diana Persa; Supervision, Antoaneta Ene; Validation, Antoaneta Ene and Marina Frontasyeva; Visualization, Marina Frontasyeva and Alina Sion; Writing – original draft, Antoaneta Ene, Florin Sloată, Marina Frontasyeva, Octavian Duliu, Alina Sion, Steluta Gosav and Diana Persa; Writing – review & editing, Antoaneta Ene, Marina Frontasyeva and Octavian Duliu. All authors read and agreed to the published version of the manuscript.

Funding: This research was funded by 2017-2022 JINR-Romania program (JINR Theme no. 03-4-1128-2017/2022; Protocol no. 4613-4-17/22 between JINR and Dunarea de Jos University of Galati), and EC through JOP Black Sea Basin 2014-2020, project code BSB27-MONITOX (2018-2021).

Data Availability Statement: Data supporting reported results are available from the corresponding author upon request.

Acknowledgments: We acknowledge the support given by JINR and IHU Kavala laboratory teams for technical support during INAA and ICP-MS analyses.

Conflicts of Interest: The authors declare no conflicts of interest. The funders had no role in the design of the study; in the collection, analyses, or interpretation of data; in the writing of the manuscript; or in the decision to publish the results.

Appendix A

Table A1. Contamination Factors (CF) for 13 PCEs in investigated soils for three layers.

Site	D (cm)	As	Cr	Cu	Cd	Co	Hg	Mn	Ni	Pb	Zn	Fe	V	Sb
G1.1	0-5	1.49	1.06	0.86	3.56	0.67	2.14	1.26	0.91	2.11	1.96	0.88	1.06	2.03
	5-20	1.65	1.03	0.68	3.22	0.89	0.69	1.18	1.36	2.77	1.76	1.11	1.05	2.45
	20-30	2.21	0.84	1.07	2.78	0.65	0.24	0.97	0.85	1.53	1.02	0.71	0.57	2.60
G1.2	0-5	2.01	1.28	0.71	3.11	0.82	0.50	0.98	1.03	1.73	2.33	1.12	0.76	2.83
	5-20	1.44	1.00	0.77	2.89	0.65	4.11	0.99	0.99	1.51	1.78	0.87	0.77	2.60
	20-30	1.65	0.94	0.75	2.56	0.71	0.69	0.86	0.98	1.41	1.26	0.78	0.63	1.95
G1.3	0-5	1.54	1.09	0.79	2.67	0.53	3.04	0.92	0.65	1.34	1.41	0.76	0.65	3.33
	5-20	1.66	0.96	1.96	2.56	0.55	2.14	1.09	0.64	1.28	1.75	1.10	0.65	2.33
	20-30	1.45	0.99	0.66	2.44	0.69	0.85	0.91	0.87	1.47	1.21	0.75	0.71	1.80
G2.1	0-5	1.68	0.80	0.49	3.78	0.40	3.75	0.91	0.35	1.44	1.12	0.56	0.68	3.23
	5-20	1.90	0.94	0.57	3.11	0.60	2.32	0.78	0.65	1.46	1.32	0.77	0.60	2.50
	20-30	1.82	1.10	0.58	2.89	0.73	0.57	0.74	0.92	0.64	1.07	0.81	0.53	2.25
G2.2	0-5	1.71	1.20	0.62	4.67	0.60	16.07	1.37	0.76	1.80	1.69	0.93	0.72	2.48
	5-20	1.76	1.28	0.76	4.33	0.62	7.50	1.05	0.71	1.62	1.41	0.89	0.72	2.33
	20-30	1.68	1.05	0.69	3.89	0.70	0.60	0.97	1.02	1.60	1.07	0.81	0.59	2.08
G2.3	0-5	2.00	1.30	0.84	5.44	0.62	0.50	1.50	0.71	3.11	3.61	1.10	0.64	4.18
	5-20	1.76	0.79	0.84	5.89	0 .58	4.16	1.08	0.75	2.19	2.22	0.66	0.85	2.38
	20-30	1.92	0.97	1.04	5.56	0.64	0.49	1.05	0.82	1.97	1.38	0.74	0.56	2.78
G3.1	0-5	2.03	1.08	0.79	2.89	0.68	0.50	0.86	0.71	1.60	1.52	0.81	0.69	2.63

 doi:10.20944/preprints202404.0668.v1

	5-20	1.73	0.98	0.78	2.78	0.66	1.13	0.83	0.85	1.37	1.07	0.71	0.58	2.30
	20-30	2.04	1.07	0.82	2.56	0.73	0.71	0.81	0.87	1.41	1.00	0.77	0.59	2.13
G3.2	0-5	2.31	1.10	0.83	6.22	0.72	2.68	1.14	0.86	2.02	1.91	1.01	0.75	3.05
	5-20	2.04	1.10	0.93	5.67	0.72	2.14	1.10	0.86	1.70	1.58	0.92	0.78	2.53
	20-30	2.10	0.93	0.86	5.22	0.68	0.65	0.90	1.00	1.77	1.06	0.79	0.58	2.10
G4.1	0-5	0.78	0.43	0.80	3.00	0.24	0.50	0.94	0.29	2.48	0.79	0.84	0.70	1.40
	5-20	1.90	0.88	0.53	2.78	0.57	2.32	0.95	0.61	1.87	1.58	0.72	0.75	3.33
	20-30	1.85	0.85	1.28	2.56	0.62	0.53	0.76	0.81	1.52	1.35	0.69	0.56	2.50
GC	0-5	1.03	0.60	0.27	1.89	0.45	0.50	0.56	0.45	0.64	0.89	0.45	0.45	1.60
	5-20	0.98	0.48	0.31	1.78	0.42	2.50	0.61	0.36	1.12	0.75	0.43	0.54	1.53
	20-30	0.83	0.46	0.09	1.56	0.39	0.35	0.45	0.26	0.53	0.45	0.35	0.32	1.38

References

1. Gonçalves, D.A.M.; Pereira, W.V.d.S.; Johannesson, K.H.; Pérez, D.V.; Guilherme, L.R.G.; Fernandes, A.R. Geochemical Background for Potentially Toxic Elements in Forested Soils of the State of Pará, Brazilian Amazon. *Minerals* **2022**, *12*, 674. https://doi.org/10.3390/min12060674
2. Zafeiriou, I.; Gasparatos, D.; Megremi, I.; Ioannou, D.; Massas, I.; Economou-Eliopoulos, M. Assessment of Potentially Toxic Element Contamination in the Philippi Peatland, Eastern Macedonia, Greece. *Minerals* **2022**, *12*, 1475. https://doi.org/10.3390/min12111475
3. Ene, A. ; Pantelică, A.; Sloată, F.; Zakaly, H.M.H.; Tekin, H.O. *Gamma spectrometry analysis of natural and man-made radioactivity and assessment of radiological risk in soils around steel industry. Rom. J. Phys.* **2023**, *68*(7–8), 803. https://doi.org/10.59277/RomJPhys.2023.68.803
4. Pantelica, A.; Freitas, M. C.; Ene, A.; Steinnes, E. Soil pollution with trace elements at selected sites in Romania studied by instrumental neutron activation analysis. *Radiochimica Acta* **2013**, *101*, 45–50. https://doi.org/10.1524/ract.2013.1989
5. Zinicovscaia, I.; Sturza, R.; Duliu, O.; Grozdov, D.; Gundorina, S.; Ghendov-Mosanu, A.; Duca, G. Major and Trace Elements in Moldavian Orchard Soil and Fruits: Assessment of Anthropogenic Contamination. *Int. J. Environ. Res. Public Health* **2020**, *17*, 7112. https://doi.org/10.3390/ijerph17197112
6. Ene, A.; Frontasyeva, M. Applications of neutron activation analysis technique in element determination at trace level. *TEHNOMUS Journal - New Technologies and Products in Machine Manufacturing Technologies* **2013**, *20*, 165–171. http://www.tehnomusjournal.fim.usv.ro/pagini/journal2013/files/28.pdf
7. Frontasyeva, M.V. Neutron activation analysis in the life sciences. *Phys. Part. Nuclei* **2011**, *42*, 332–378. https://doi.org/10.1134/S1063779611020043
8. Abdushukurov, D.A.; Abdusamadzoda, D.; Zinicovscaia, I.; Duliu, O.G.; Nekhoroshkov, P.S. On the geochemistry of major and trace elements distribution in sediments and soils of Zarafshon River Valley, Western Tajikistan. *Appl. Sci.* **2022**, *12*, 2763 (2022). https://doi.org/10.3390/app12062763
9. Badawy, W.M.; Duliu, O.G.; El Samman, H.; El-Taher, A.; Frontasyeva, M.V. A review of major and trace elements in Nile River and Western Red Sea sediments: An approach of geochemistry, pollution, and associated hazards. *Appl. Radiat. Isot.* **2021**, *170*, 109595. https://doi.org/10.1016/j.apradiso.2021.109595
10. Ene, A.; Pantelica, A.; Freitas, C.; Bosneaga, A. EDXRF and INAA analysis of soils in the vicinity of a metallurgical plant. *Rom. Journ. Phys.* **2011**, *56*, 993–1000. https://rjp.nipne.ro/2011_56_7-8/0993_1000.pdf
11. Ene, A.; Bosneaga, A.; Georgescu, L. Determination of heavy metals in soils using XRF technique. *Rom. Journ. Phys*. **2010**, *55*, 815–820. https://rjp.nipne.ro/2010_55_7-8/0815_0820.pdf
12. El-Taher, A.; Ashry, A.; Ene, A.; Almeshari, M.; Zakaly, H.M.H. Determination of phosphate rock mines signatures using XRF and ICP-MS elemental analysis techniques: radionuclides, oxides, rare earth, and trace elements. *Rom. Rep. Phys.* **2023**, *75*(2), 701. https://rrp.nipne.ro/2023/AN75701.pdf
13. Awad, H.A.; El-Leil, I.A.; Granovskaya, N.V., Ene, A.; Tolba, A.; Kamel, M ; Nastavkin, A.; El-Wardany, R. M.; Zakaly, H.M.H. Petrotectonic and geochemistry of Abu Murrat ilmenite bearing gabbro, NE Desert, Egypt, *Rom. J. Phys.* **2022**, *67*(5–6), 808.
14. Sloata, F.; Ene, A.; Bogdevici, O.; Spanos, T. Characterization of soils around a former chemical plant in Braila, SE Romania, using high performance atomic techniques (EDXRF, AAS, ICP-MS). *Ann. Dunarea de Jos Univ. Galati, Fasc. II, Math. Phys. Theor. Mech.* **2022**, *45*, 23–32. https://doi.org/10.35219/ann-ugal-math-phys-mec.2022

15. Teodorof, L.; Burada, A.; Despina, C.; Seceleanu-Odor, D.; Spiridon, C.; Țigănuș, M.; Tudor, M.I.; Tudor, M.; Ene, A.; Zubcov, E.; Spanos, T.; Bogdevich, O. Sediments quality assessment in terms of single and integrated indices from Romanian MONITOX network (2019 – 2020). *Ann. Dunarea de Jos Univ. Galati, Fasc. II, Math. Phys. Theor. Mech.* **2020**, *43*(2) 175–183. https://doi.org/10.35219/ann-ugal-math-phys-mec.2020.2.16
16. Bosneaga (Sion), A. Quantification of the soil pollution level (Cuantificarea gradului de poluare a solului – in Romanian), PhD Thesis, Dunarea de Jos University of Galati, Romania, 2011.
17. Ene, A.; Bogdevich, O.; Sion, A. Levels of organochlorine pesticides (OCPs) and polycyclic aromatic hydrocarbons (PAHs) in topsoils from SE Romania. Sci. Total Environ. **2012**, 439, 76–86. https://doi.org/10.1016/j.scitotenv.2012.09.004
18. Popescu, I.; Badica, T.; Olariu, A.; Besliu, C.; Ene, A.; Ivanescu, A. Multielemental analysis of metallurgical samples by thermal neutron activation. *J. Radioanal. Nucl. Chemistry* **1996**, *213*, 369–376. https://doi.org/10.1007/BF02162935
19. Ene, A.; Popescu, I. V.; Ghisa, V. Study of transfer efficiencies of minor elements during steelmaking by neutron activation technique. *Rom. Rep. Phys.* **2009**, *61*, 165–171. https://rrp.nipne.ro/2009_61_1/art14Ene.pdf
20. Ene, A., Pantelica, A.: Study of transfer of minor elements during ironmaking by neutron activation analysis. Radiochim. Acta **201**0, *98*, 53–57. https://doi.org/10.1524/ract.2010.1685
21. Moraru, S.-S.; Ene, A.; Badila, A. Physical and Hydro-Physical Characteristics of Soil in the Context of Climate Change. A Case Study in Danube River Basin, SE Romania. *Sustainability* **2020**, *12*, 9174. https://doi.org/10.3390/su12219174
22. Chițescu, C.L.; Ene, A.; Geana, E.-I.; Vasile, A.M.; Ciucure, C.T. Emerging and Persistent Pollutants in the Aquatic Ecosystems of the Lower Danube Basin and North West Black Sea Region—A Review. *Appl. Sci.* **2021**, 11(20), 9721. https://doi.org/10.3390/app11209721
23. Sloată, F. Performant analytical techniques used for toxic substances monitoring and industrial waste management (Tehnici analitice performante utilizate pentru monitorizarea substanțelor toxice și managementul deșeurilor industriale – in Romanian), PhD Thesis, Dunarea de Jos University of Galati, Romania, 2023.
24. Ene, A.; Zubcov, E.; Spanos, T.; Bogdevich, O.; Teodorof, L. MONITOX international network for monitoring of environmental toxicants and risk assessment in the Black Sea Basin: research and interdisciplinary cooperation dimensions. In Proceedings of the 10th International Conference "Sustainable use and protection of animal world in the context of climate change", Chisinau, Moldova, 16-17 September 2021, pp. 11–17. https://doi.org/10.53937/icz10.2021.01
25. Frontasyeva, M.V. Epithermal Neutron Activation Analysis at the IBR-2 reactor of the Frank Laboratory of Neutron Physics at the Joint Institute for Nuclear Research (Dubna). *Phys. Atom. Nuclei* **2008**, *71*, 1684–1693. https://doi.org/10.1134/S1063778808100049
26. Pavlov, S.S.; Dmitriev, A.Y.; Frontasyeva, M.V. Automation system for neutron activation analysis at the reactor IBR-2, Frank Laboratory of Neutron Physics, Joint Institute for Nuclear Research, Dubna, Russia. *J. Radioanal Nucl. Chem.* **2016**, *309*, 27–38. https://doi.org/10.1007/s10967-016-4864-8
27. Badawy, W.M.; Ghanim, E.H.; Duliu, O.G.; El Samman, H.; Frontasyeva, M.V. Major and trace element distribution in soil and sediments from the Egyptian central Nile Valley. *Journal of African Earth Sciences* **2017**, *131*, 53–61. https://doi.org/10.1016/j.jafrearsci.2017.03.029
28. Arafa, W.M.; Badawy, W.M.; Fahmi, N.M.; Ali, K.; Gad, M.S.; Duliu, O.G.; Frontasyeva, M.V.; Steinnes, E. Geochemistry of sediments and surface soils from the Nile Delta and lower Nile valley studied by Epithermal Neutron Activation Analysis. *Journal of African Earth Sciences* **2015**, *107*, 57–64. https://doi.org/10.1016/j.jafrearsci.2015.04.004
29. Dorronsoro, C.; Martin, F.; Garcia, I.; Simon, M.; Fernandez, E.; Aguilar, J.; Fernandez, J. Migration of trace elements from pyrite tailings in carbonate soils. J. Environ. Qual. **2002**, *31*, 829–835. https://doi.org/10.2134/jeq2002.8290
30. Sion (Bosneaga), A.; Ene, A.; Georgescu, L.P. Heavy metals in soils near an industrial plant in Galati, Romania: implications for the population health risk. *J. Sci. Arts* **2011**, *3*(16) 299–302. https://josa.ro/docs/josa_2011_3/b.02_Alina_Sion.pdf
31. Håkanson, L. An Ecological Risk Index for Aquatic Pollution Control: A Sedimentological Approach. *Water Research* **1980**, *14*, 975–1101. https://doi.org/10.1016/0043-1354(80)90143-8

32. Kowalska, J.B.; Mazurek, R.; Gasiorek, M.; Zaleski, T. Pollution indices as useful tools for the comprehensive evaluation of the degree of soil contamination–A review. *Environ. Geochem. Health* **2018**, *40*, 2395–2420. https://doi.org/10.1007/s10653-018-0106-z
33. Sur, I.M.; Micle, V.; Polyak, E.T.; Gabor, T. Assessment of soil quality status and the ecological risk in the Baia Mare, Romania Area. *Sustainability* **2022**, *14*, 3739. https://doi.org/10.3390/su14073739
34. Kumar, V.; Pandita, S.; Setia, R. A meta-analysis of potential ecological risk evaluation of heavy metals in sediments and soils. *Gondwana Research* **2022**, *103*, 487–501. https://doi.org/10.1016/j.gr.2021.10.028
35. Tomlinson, D.L.; Wilson, J.G.; Harris, C.R.; Jeffrey, D.W. Problems in the assessment of heavy-metal levels in estuaries and the formation of a pollution index. *Helgolander Meeresunters* **1980**, *33*, 566–575. https://doi.org/10.1007/BF02414780
36. Order of the Minister of Water, Forests and Environmental Protection no. 756/03.11.1997 for the approval of the Regulation regarding the assessment of environmental pollution, Official Monitor of Romania no. 303bis from 6 November 1997.
37. Shi, J.; Zhao, D.; Ren F.; Huang, L. Spatiotemporal variation of soil heavy metals in China: The pollution status and risk assessment. *Science of the Total Environment* **2023**, *871*, 161768. http://dx.doi.org/10.1016/j.scitotenv.2023.161768
38. Badawy, W.M.; El-Taher, A.; Frontasyeva, M.V.; Madkour, H.A.; Khater, A.E.M. Assessment of anthropogenic and geogenic impacts on marine sediments along the coastal areas of Egyptian Red Sea. *Applied Radiation and Isotopes* **2018**, *140*, 314–326. https://doi.org/10.1016/j.apradiso.2018.07.034
39. Spatial Analyst in ArcGIS for Desktop 10.4. https://www.esri.com/arcgis-blog/products/analytics/analytics/spatial-analyst-in-arcgis-for-desktop-10-4/
40. Burrough, P.A.; McDonnell, R.A.; Lloyd, C.D. Principles of geographical information systems, Oxford University Press, 2015, ISBN 9780198742845
41. Blebea-Apostu, A.-M.; Margineanu, R.M.; Persa, D.; Dumitras, D.-G.; Gomoiu, M.C.; Duliu, O.G. The distribution of natural radionuclides ^{40}K, ^{228}Ac, and ^{226}Ra on Romanian Territory: a radiometric study. *Environ. Monit. Assess.* **2024**, *196*, 186. https://doi.org/10.1007/s10661-024-12374-y
42. Shepard, D. A two-dimensional interpolation function for irregularly-spaced data. In *Proceedings of the 1968 ACM National Conference,* pp. 517–524, https://dl.acm.org/doi/pdf/10.1145/800186.810616 (accessed 22.02.2024)
43. Spatial Autocorrelation (Global Moran's I) (Spatial Statistics). https://pro.arcgis.com/en/pro-app/latest/tool-reference/spatial-statistics/spatial-autocorrelation.htm
44. McLachlan, G.J. Discriminant Analysis and Statistical Pattern Recognition. Wiley Interscience, 2004, ISBN 978-0-471-69115-0.
45. https://past.en.lo4d.com/windows
46. StatSoft, Inc. STATISTICA 11. www.statsoft.com.
47. OriginLab Corporation, https://www.originlab.com/2021
48. Rudnick, R.L.; Gao, S. Composition of the continental crust. In Treatise on Geochemistry; Holland, H.D., Turekian, K.K., Eds.; Elsevier-Pergamon: Amsterdam, The Netherlands, 2004; Volume 3, pp. 1–64, ISBN 978-0-08-098300-4.
49. Marshak, S. Essentials of Geology, 6th ed.;W.W. Norton & Company: New York, NY, USA, 2019; ISBN 978-0393667523
50. Norman, J.C.; Haskin, L.A. The geochemistry of Sc: A comparison to the rare earths and Fe. *Geochimica et Cosmochimica Acta* **1968**, *32*, 93–108, https://doi.org/10.1016/0016-7037(68)90089-6
51. Armstrong, A.J.S.; Nagarajan, R.; Madhavaraju, J. et al.. Geochemistry of the Jurassic and Upper Cretaceous shales from the Molango Region, Hidalgo, eastern Mexico: Implications for source-area weathering, provenance, and tectonic setting. *Comp. Ren. Geosci.* **2013**, *45*, 185–202. https://doi.org/10.1016/j.crte.2013.03.004
52. McLennan, S.M.; Hemming, S.; McDaniel, D.K.; et al.. Geochemical Approaches to Sedimentation, Provenance, and Tectonics; Special paper; Geological Society of America: Boulder, CO, USA, 1993; Volume 284, p. 20.
53. Tugulan L.C.; Duliu O.G.; Bojar A-V.; et al. On the geochemistry of the Late Quaternary loess deposits of Dobrogea (Romania). *Quaternary International* **2016**, *399*, 100–110. https://doi.org/10.1016/j.quaint.2015.06.062

 doi:10.20944/preprints202404.0668.v1

54. Taylor, S.R.; McLennan, S.M.; The Continental Crust: Its Composition and Evolution. Blackwell, Oxford, 1985.
55. Gromet, L.P.; Haskin, L.Y.; Korotev, R.L.; et al. The North American shale composite: Its compilation, major and trace element characteristics. *Geochimica et Cosmochimica Acta* **1984**, *48*, 2469–2482,. https://doi.org/10.1016/0016-7037(84)90298-9